JOURNAL OF VIROLOGY, Apr. 1997, p. 2947–2958 Vol. 71, No. 4
0022-538X/97/$04.00+0

Association of Influenza Virus NP and M1 Proteins with Cellular Cytoskeletal Elements in Influenza Virus-Infected Cells

ROY T. AVALOS, ZHONG YU, AND DEBI P. NAYAK*

Department of Microbiology and Immunology, Jonsson Comprehensive Cancer Center, UCLA School of Medicine, Los Angeles, California 90095-1747

Received 28 October 1996/Accepted 23 December 1996

We have investigated the association of the influenza virus matrix (M1) and nucleoprotein (NP) with the host cell cytoskeletal elements in influenza virus-infected MDCK and MDBK cells. At 6.5 h postinfection, the newly synthesized M1 was Triton X-100 (TX-100) extractable but became resistant to TX-100 extraction during the chase with a $t_{1/2}$ of 20 min. NP, on the other hand, acquired TX-100 resistance immediately after synthesis. Significant fractions of both M1 and NP remained resistant to differential detergent (Triton X-114, 3-[(3-cholamidopropyl)dimethylammonio]-1-propanesulfonate [CHAPS], octylglucoside) extraction, suggesting that M1 and NP were interacting with the cytoskeletal elements. However, the high-molecular-weight form of the viral transmembrane protein hemagglutinin (HA), which had undergone complex glycosylation, also became resistant to TX-100 extraction but was sensitive to octylglucoside detergent extraction, indicating that HA, unlike M1 or NP, was interacting with TX-100-insoluble lipids and not with cytoskeletal elements. Morphological analysis with cytoskeletal disrupting agents demonstrated that M1 and NP were associated with microfilaments in virus-infected cells. However, M1, expressed alone in MDCK or HeLa cells from cloned cDNA or coexpressed with NP, did not become resistant to TX-100 extraction even after a long chase. NP, on the other hand, became TX-100 insoluble as in the virus-infected cells. M1 also did not acquire TX-100 insolubility in *ts* 56 (a temperature-sensitive mutant with a defect in NP protein)-infected cells at the nonpermissive temperature. Furthermore, early in the infectious cycle in WSN-infected cells, M1 acquired TX-100 resistance very slowly after a long chase and did not acquire TX-100 resistance at all when chased in the presence of cycloheximide. On the other hand, late in the infectious cycle, M1 acquired TX-100 resistance when chased in either the presence or absence of cycloheximide. Taken together, these results demonstrate that M1 and NP interact with host microfilaments in virus-infected cells and that M1 requires other viral proteins or subviral components (possibly viral ribonucleoprotein) for interaction with host cytoskeletal components. The implication of these results for viral morphogenesis is discussed.

Influenza viruses assemble and bud from the plasma membrane of infected cells and predominantly from the apical domain of the plasma membrane in polarized epithelial cells (47). However, little is known about the steps involved in the assembly and budding of influenza viruses. For virus budding to occur, all viral structural components including the nucleocapsid (RNP), matrix protein (M1), and envelope proteins (HA, NA, M2) must be transported either individually or as subviral components to the assembly site at the plasma membrane (47). These viral proteins and/or subviral components must then interact with each other to initiate the budding processes leading to the morphogenesis and release of virions. One of our major interests is to elucidate the processes involved in bringing the viral components to the assembly site in virus-infected cells. Over the last few years, we have been studying the assembly of orthomyxo- and paramyxoviruses, including the transport and sorting of influenza virus glycoproteins, namely, viral hemagglutinin (HA) and neuraminidase (NA) (28, 48), the role of M1 in the nuclear exit of viral RNP (55), abortive assembly in influenza virus-infected HeLa 229 cells (18), and the interaction between the matrix (M) protein and glycoproteins (F and HN) of Sendai virus (61).

Influenza virus M1 is the most abundant protein in virus particles and appears to play a central role in the assembly and budding processes. Although neither glycoprotein (HA or NA) is absolutely required for assembly and budding processes (34, 35, 42, 51), virus assembly and budding fail to occur in the absence of M1 (36). Particle formation is drastically reduced in abortively infected cells exhibiting reduced M1 synthesis and in cells infected at the nonpermissive temperature with temperature-sensitive (*ts*) virus with a defect in M1 protein (33, 74). Because of the presumed juxtaposition of M1 protein between the viral envelope and nucleocapsid, M1 is proposed to interact with the lipid bilayer and/or transmembrane domain/cytoplasmic tail of viral glycoprotein(s) on one side and the components of viral ribonucleoproteins (vRNP) on the other side (19, 25, 40, 46). Recently, interactions of influenza virus and Sendai virus matrix proteins with viral glycoproteins facilitating membrane binding of matrix proteins has been demonstrated (10, 61). However, how the M1 is brought to the assembly site remains unknown.

Since cytoskeletal components of host cells are involved in protein transport and RNA sorting (20, 30, 49, 69), we have examined their role in the viral assembly and budding processes. Cytoskeletal components undergo alteration during virus infection (8, 57, 71) and appear to be involved in virus assembly and budding of enveloped viruses including orthomyxo- and paramyxoviruses (4, 13, 16). Drugs disrupting cytoskeletal components (actin and microtubule) affect the polarized transport of viral HA (56). Immunofluorescence studies have suggested the colocalization of actin and M1 in influenza virus-infected CV-1 cells (6). Triton X-100 (TX-100) detergent extraction of virus-infected cells has indicated a possible interaction of HA with cytoskeletal components in

* Corresponding author. Phone: (310) 825-8558. Fax: (310) 206-3865.

MDCK cells (66). However, these studies did not distinguish between the interaction of viral components with TX-100-insoluble lipids and TX-100-insoluble cytoskeletal components. Consequently, the nature and function of such interaction in the sorting and transport of viral proteins and in viral morphogenesis including assembly and budding are not known. As a step toward understanding the processes involved in virus assembly and the role of host components in viral morphogenesis, we have initiated studies to investigate the interaction of viral components with the host membrane and cytoskeleton. In this study, we have examined the complex interaction of M1 and NP with cytoskeletal components in influenza virus-infected cells.

MATERIALS AND METHODS

Cells, virus, and antibodies. Madin-Darby bovine kidney (MDBK) and Madin-Darby canine kidney (MDCK) cells were obtained from the American Type Tissue Culture Collection and maintained as previously described (51). Temperature-sensitive (*ts*) mutants of WSN virus were plaque purified and grown at the permissive temperature (33°C) as reported previously (27, 63). Influenza virus A/WSN/33 (H1N1) was plaque purified on MDBK cells, and virus stocks were made from individual plaques as previously described (51). PFU and hemagglutination (HA) units were determined as described previously (51). Typical titers of virus stocks ranged from 5×10^7 to 5×10^8 PFU/ml. The vaccinia virus recombinant VP273-expressing M1 protein was obtained from E. Paleotti and propagated as reported previously (6); it had a titer of 2×10^8 pfu in CV-1 cells. Transfected MDCK cells stably expressing M1 were obtained as described previously (28). Briefly, a cDNA encoding the A/PR/8/34 M1 was cloned under the control of the metallothionein promoter of pMEP4 (Invitrogen, San Diego, Calif.). Hygromycin-resistant clones were selected, and M1 was expressed by induction with Cd^{2+} and analyzed by immunofluorescence and immunoprecipitation assays. Polyclonal anti-WSN antibodies were made in rabbits by using purified virus. Monoclonal anti-M1 antibodies were obtained from Brian Murphy (National Institute of Allergy and Infectious Diseases), and polyclonal anti-NS1 antibodies were a gift of Peter Palese (Mt. Sinai). Monoclonal anti-tubulin, anti-vimentin, and anti-actin antibodies were purchased from Sigma.

Radiolabeling and immunoprecipitation. Influenza virus (10 PFU/cell) was adsorbed to 5×10^6 MDBK cells for 1 h at room temperature. The infected cells were then incubated at 37°C in Dulbecco's minimal essential medium (DMEM) plus 2.5% fetal bovine serum (FBS). At the indicated time postinfection (p.i.), cells were starved in MEM minus methionine and cysteine for 30 min and labeled for 15 min with 100 μCi each of [^{35}S]Translabel and [^{35}S]cysteine per ml. Labeling medium was then replaced with the chase medium (MEM supplemented with 2.5% FBS, 10 mM cysteine, and 10 mM methionine) and chased for various times. The cells were then either extracted with TX-100 detergent or fractionated into nuclear and cytoplasmic fractions. Each fraction was then diluted 10-fold with RIPA buffer (50 mM Tris [pH 7.5], 150 mM NaCl, 1.0% TX-100, 0.5% sodium deoxycholate, 0.1% sodium dodecyl sulfate [SDS], 1.0 mM phenylmethylsulfonyl fluoride) and incubated at 4°C with gentle shaking for 30 min. The samples were cleared by centrifugation at $1,000 \times g$ for 5 min. Upon the addition of anti-WSN rabbit polyclonal antibodies, samples were incubated further for 2 h at 4°C. Subsequently, 7.5 mg of protein A-Sepharose (Pharmacia) was added to each sample, and the mixture incubated for 1.5 h at 4°C. The immunoprecipitates bound to Sepharose beads were pelleted by centrifugation and washed in 1.0 ml of RIPA buffer containing 5 mg of bovine serum albumin per ml, followed by another wash with 1.0 ml of RIPA buffer. Immunoprecipitates were then dissolved in SDS sample buffer (50 mM Tris-HCl [pH 6.8], 5% 2-mercaptoethanol, 2% SDS, 10% [wt/vol] glycerol, 0.1% [wt/vol] bromophenol blue) at 95°C for 5 min and analyzed by 1% SDS–polyacrylamide gel electrophoresis (PAGE) (10% polyacrylamide) (29).

Nuclear and cytoplasmic fractionation. The procedures used for nuclear and cytoplasmic fractionation of virus-infected cells were essentially the same as reported previously (55), with a few modifications. Briefly, infected cells were scraped into 1.0 ml of phosphate-buffered saline containing Ca^{2+} and Mg^{2+} (PBS^{2+}) and pelleted at $1,000 \times g$ for 5 min. The resulting cell pellet was resuspended in TMN buffer (10 mM Tris-HCl [pH 7.2], 3.0 mM $MgCl_2$, 140 mM NaCl, 1.0% Nonidet P-40, 1.0% TX-100, 0.5% sodium deoxycholate) plus aprotinin (100 kallekrein units/ml [final concentration]) and incubated on ice for 30 min. The cell preparation was then passed through a 26-gauge hypodermic needle 20 times and centrifuged for 5 min at $1,000 \times g$. For Western blot analysis, aliquots of the supernatant (cytoplasmic) and the pellet (nuclear) fractions were resuspended in SDS sample buffer and used for SDS-PAGE analysis. For immunoprecipitation, the nuclear fraction was incubated for 10 min at 95°C and then passed through a 26-gauge needle another 20 times and centrifuged at $1,000 \times g$ for 5 min to remove the insoluble debris. The nuclear and cytoplasmic fractions were diluted 20-fold with RIPA buffer and immunoprecipitated with specific antibodies as described above.

Detergent extraction. Two procedures were used for detergent extraction. In one, virus-infected cell monolayers were extracted directly on tissue culture plates by a modified procedure of Morrison and McGinnes (43). Briefly, cell monolayers were washed twice with 1.0 ml of ice-cold PBS^{2+} and then once with 1.0 ml of extraction buffer (EB) (0.05 M NaCl, 0.003 M KCl, 0.01 M HEPES [pH 7.4], 2.5 mM $MgCl_2$, 0.3 M sucrose). The monolayers were then extracted on ice with 0.5 ml of EB containing 1.0% TX-100 with intermittent rocking for 20 min, and the supernatant (TX-100-soluble fraction) was removed directly from the culture dish. The remaining insoluble cellular material was washed once with DDB (10 mM NaCl, 1.5 mM $MgCl_2$, 10 mM Tris-HCl [pH 7.5]) without detergent, resuspended in 0.5 ml of DDB containing 1% Tween 40 and 0.5% sodium deoxycholate, incubated for 5 min on ice, and subsequently passed through a 26-gauge needle 20 times. Nuclei appeared intact and free from membranous and cytoskeletal components when examined by light microscopy. The cell material was then centrifuged for 5 min at $1,000 \times g$ to separate the cytoskeletal framework (supernatant) from the nuclei (pellet). We also analyzed the recovery of total proteins in the TX-100-soluble and insoluble fractions by using parallel dishes, one for TX-100 extraction and the other for total proteins. We observed that the combined recovery of viral proteins in both TX-100-soluble (S) and insoluble (I) samples was over 90% of the total (data not shown). The percentage of proteins present in S and I fractions was calculated from the amount of total proteins present in S and I fractions. In the other procedure, modified from that of Brown and Rose (5), cells were scraped into EB without detergent, mixed gently with an equal volume of EB containing 2% TX-100, and incubated in ice for 5 min. The mixture was then centrifuged at $1,000 \times g$ for 5 min to isolate the TX-100-soluble fraction. The pellet fraction was treated with DDB containing 1% Tween 40 and 0.5% sodium deoxycholate as above to separate the cytoskeletal component from nuclei. Both procedures yielded similar results.

Western blot analysis. Samples were separated under reducing conditions by SDS-PAGE (10% polyacrylamide) in a minigel apparatus (Bio-Rad) before overnight electrotransfer (250 mA) onto nitrocellulose membranes (Schleicher & Schuell) in a blotting buffer (25 mM Tris-HCl [pH 7.2], 190 mM glycine, 20% methanol). The membranes were then incubated for 30 min in blocking buffer (WBB) (50 mM Tris-HCl [pH 7.5], 150 mM NaCl, 0.05% Tween 20, 3% [vol/vol] nonfat milk). They were subsequently incubated with either an anti-M1, anti-actin, or anti-HA monoclonal antibodies for 1 h and washed three times with WBB. Finally, a WBB solution containing secondary alkaline phosphatase-conjugated goat anti-mouse antibodies (Cappel) was applied to the membranes for 1 h. The membranes were developed with 5-bromo-4-chloro-3-indolylphosphate toluidinium–nitroblue tetrazolium (BCIP/NBT) phosphatase substrate (Kirkegaard & Perry Laboratories, Inc.) diluted 1:2 in 100 mM Tris-HCl (pH 9.5).

Indirect immunofluorescent staining. MDBK cells (4×10^5) were grown overnight in tissue culture chamber slides (Nunc) and synchronously infected with WSN virus at a multiplicity of infection (MOI) of 5 for 1.0 h at 4°C. Subsequently, 1.5 ml of prewarmed (37°C) DMEM containing 2.5% FBS was added to the cell monolayers for 7.0 h. Infected cells were then fixed with 100% acetone at −20°C for 20 min and stained with anti-M1, anti-NP, anti-tubulin, and anti-vimentin monoclonal antibodies (55). Filamentous actin was stained with rhodamine-phalloidin (Molecular Probes Inc.) as described previously (1). Cellular actin was disrupted with cytochlasin D (Sigma) as described previously (7).

Northern blot analysis. A plus-strand-specific ^{32}P-labeled riboprobe was transcribed from a PR8 M1 viral cDNA clone (provided by Peter Palese) by T7 RNA polymerase as suggested by the supplier (Promega). Total cellular RNA was extracted from 5×10^6 MDBK cells infected with WSN virus at an MOI of 10 at the specific time postinfection by the hot-phenol method (58). The RNA was fractionated in a 1% agarose gel and denatured in situ for subsequent blotting onto a nytran membrane (Schleicher & Schuell) as described previously (58). The blot was prehybridized for 2 h at 42°C in a hybridization buffer containing 50% formamide and then hybridized with the labeled probe at the same temperature overnight. Subsequently, the blot was washed three times for 20 min at room temperature with 1× SSC (0.15 M NaCl plus 0.015 M sodium citrate)–0.1% SDS at room temperature for 20 min each. The membrane was washed three more times in 0.1× SSC at 52°C for 20 min each (58). The hybridization signal was then detected by autoradiography.

RESULTS

Nuclear-cytoplasmic distribution of M1 and NP in influenza virus-infected MDBK cells. Influenza virus M1 and NP are present in both the nucleus and cytoplasm (6, 50) and appear to possess nuclear targeting signals (75). However, the nuclear and cytoplasmic localizations of M1 and NP appears to depend on the time of the infectious cycle, i.e., early versus late (55, 72), and modifications such as phosphorylation (73). Since in this study we wanted to investigate the interactions of cytoplasmic M1 and NP with host components, we examined the cytoplasmic and nuclear distribution of M1 and NP in virus-infected cells. Accordingly, MDBK cells were infected with WSN virus at an MOI of 10 and separated into nuclear and cyto-

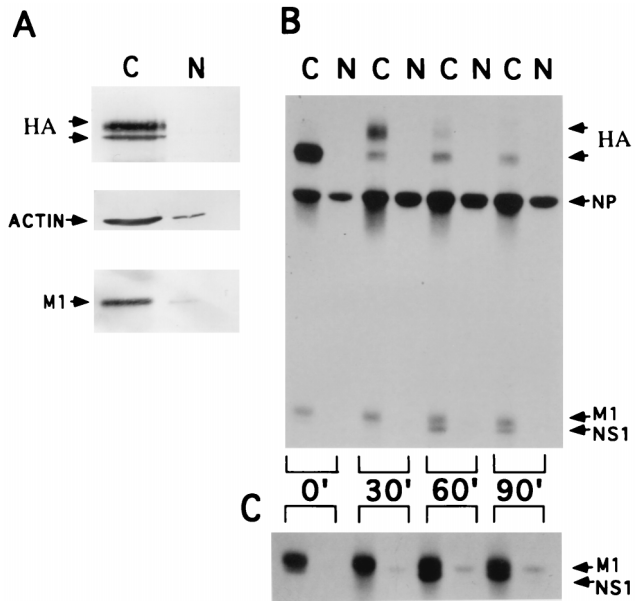

FIG. 1. Cytoplasmic and nuclear fractionation of WSN-infected MDBK cells. Monolayers of MDBK cells (5×10^6) were infected with WSN virus at an MOI of 10. (A) At 7 h p.i., infected cells were harvested and fractionated into nuclear (N) and cytoplasmic (C) fractions, analyzed by SDS-PAGE, and subjected to Western blot analysis with monoclonal anti-HA (HA), anti-actin (actin), or anti-M1 (M1) antibodies. (B) For pulse-chase experiments, infected cells were labeled for 15 min with [^{35}S]cysteine (100 μCi) and [^{35}S]Translabel (100 μCi) at 7 h p.i. and chased for various times. Nuclear and cytoplasmic fractions were then subjected to immunoprecipitation with polyclonal anti-WSN rabbit antibodies, and immunoprecipitates were analyzed by SDS-PAGE as described in Materials and Methods. (C) Overexposure of M1 and NS1 in panel B.

plasmic fractions at 7 h p.i. as described in Materials and Methods. The nuclear and cytoplasmic fractions were analyzed for cellular actin and viral HA and M1 by Western immunoblotting with monoclonal antibodies against actin, HA, or M1. We observed that when fractionation was performed with EB containing 1% Nonidet-40, 1% TX-100, and 0.5% sodium deoxycholate along with a homogenization step through a 26-gauge needle, nuclear fractions were essentially free from cytoskeletal or membrane structures. Western blot analysis (Fig. 1A) showed that nuclear fractions did not contain any influenza virus HA and contained only trace amounts (<10%) of cellular actin. Over 90% of the M1 protein fractionated with the cytoplasmic fraction, while only a minor population (<10%) appeared in the nuclear fraction (Fig. 1A). These results show that at 7 h p.i. the majority of M1 protein was present in the cytoplasmic compartment of WSN-infected MDBK cells.

To determine the time necessary to reach the steady-state distribution of M1 and NP in the cytoplasmic and nuclear compartments, we performed pulse-chase experiments. Accordingly, virus-infected cells at 7 h p.i. were pulse-labeled for 15 min and chased for various periods as described in Materials and Methods. The cells were harvested after specified chase periods and fractionated into cytoplasmic and nuclear fractions. The fractions were immunoprecipitated with anti-WSN polyclonal antibodies and analyzed by SDS-PAGE (10% polyacrylamide). Initially, the labeled M1 protein was found only within the cytoplasmic fraction (Fig. 1B, 0′), but with chase, a small fraction (<10%) of the labeled M1 appeared in the nucleus and reached a steady state by 60 to 90 min (Fig. 1C). These results were similar to the ratios of nuclear and cytoplasmic M1 obtained by Western blotting (Fig. 1A) and show that at 7 h p.i. a steady-state distribution of the nuclear and cytoplasmic M1 protein was reached by approximately 90 min after its synthesis and that the major population of M1 protein was present in the cytoplasm late in the infectious cycle. The labeled NS1 was found only in the cytoplasmic fraction even though NS1 is a nuclear protein and is abundantly found in the nucleus (15). Since the whole virus antibodies used in these experiments did not contain anti-NS1 antibodies, the presence of NS1 in the cytoplasmic fraction would indicate complex formation between NS1 and one or more viral components in the cytoplasm. Although NS1 was prominent in the cytoplasmic fraction at 60 min of chase, it was also present at earlier times of chase, as evident from a longer exposure (Fig. 1C). The presence of NS1 in the immunoprecipitate was identified by Western blot analysis of the immunoprecipitate with polyclonal anti-NS1 antibodies (data not shown). Unlike M1, a significant fraction of NP (15 to 20%) was found in the nucleus within the pulse time and increased to 40% by 60 min of chase (Fig. 1B). Thus, the kinetics of nuclear translocation of M1 and NP were different in virus-infected cells, as reported previously (72).

Interaction of WSN M1 with cytoskeletal components. To determine if influenza virus proteins were associated with cytoskeletal elements, we extracted virus-infected cells with nonionic detergents. Monolayers of WSN-infected MDBK cells at 7 h p.i. were extracted with TX-100 to isolate the TX-100-soluble, TX-100-insoluble, and nuclear fractions as described in Materials and Methods and analyzed by Western blotting (Fig. 2A). The cytoplasmic TX-100-resistant component has been operationally defined as the cytoskeletal framework (3, 26, 43). The extraction procedure used in this study shows that approximately 50% of the actin existed as the soluble form (g actin) and the remaining 50% existed as the filamentous TX-100-insoluble form (f actin), as has been reported for nonmuscle cells (59), and, again, none was present in the nuclear fraction (Fig. 2A), even after overstaining (data not shown). In preliminary experiments to optimize the extraction procedure, the extraction period and TX-100 concentration were varied. Essentially, similar results were obtained whether the cells were incubated with TX-100 for 2, 5, 10, or 20 min or with different concentrations (0.25, 0.5, and 1.0%) of TX-100 (data not shown). Therefore, to ensure complete extraction, the cell monolayers were treated with 1% TX-100 for 20 min in all experiments unless otherwise specified. The results were similar when the TX-100 extraction procedure of Brown and Rose (5) was used (data not shown).

The results of the Western blot analysis also show that the nuclear fraction was free from any HA and actin, as expected (Fig. 2A). The TX-100-insoluble fraction contained higher-molecular-weight HA, while the lower-molecular-weight HA was present predominantly in the TX-100-soluble fraction (Fig. 2A). These results agree with the previous data that only the HA which had undergone complex glycosylation and acquired higher molecular weight and exhibited endo-β-*N*-acetylglucosaminidase H resistance became resistant to TX-100 extraction (66). The M1 protein, predominantly present in the cytoplasmic fractions, was essentially distributed equally between the TX-100-soluble and -insoluble fractions. Again, only a minor population of the M1 protein was found in the nuclear fraction. These results show that in virus-infected cells at 7 h p.i., the cytoplasmic M1 (Fig. 2A) and NP (data not shown) proteins existed in two different populations: TX-100-soluble and TX-100-insoluble M1.

Pulse-chase experiments were then performed to determine the kinetics by which the M1 and NP proteins acquired resis-

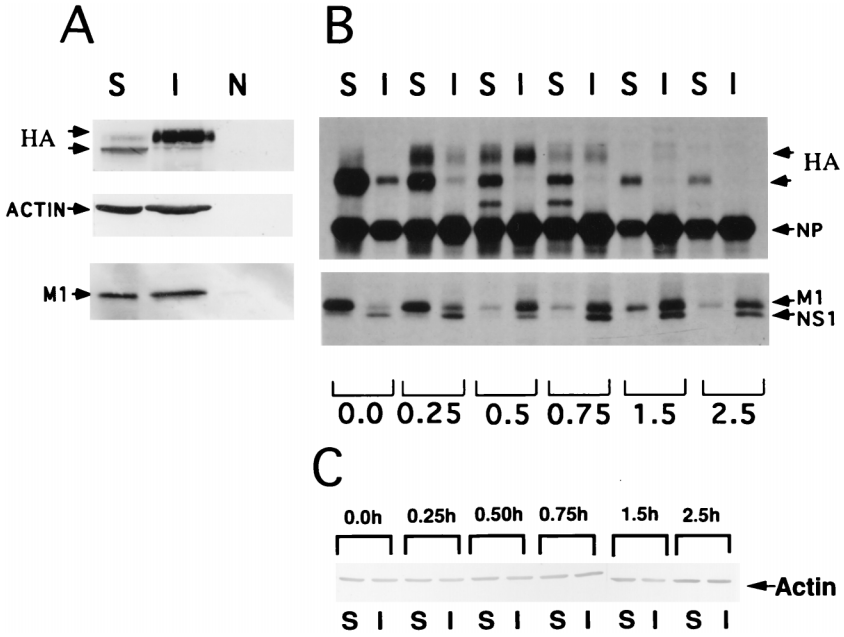

FIG. 2. TX-100 detergent extraction of WSN-infected MDBK cells. (A) At 7 h p.i., virus-infected cells were subjected to TX-100 extraction as described in Materials and Methods and fractionated into TX-100-soluble (S), TX-100-insoluble (I), and nuclear (N) fractions. For Western blot analysis, fractions were analyzed by SDS-PAGE, blotted, and incubated with either anti-HA (HA), anti-actin (actin), or anti-M1 (M1) monoclonal antibodies. The nuclear fraction did not contain either of these proteins, and the TX-100-insoluble fraction (I) contained predominantly the high-molecular-weight HA. (B) For pulse-chase analysis, WSN-infected cells at 6.5 h p.i. were labeled for 15 min with [^{35}S]cysteine (100 μCi) and [^{35}S]Translabel (100 μCi) and chased for various times. Cells were then fractionated into TX-100-soluble (S), TX-100-insoluble (I), and nuclear fractions. The TX-100-soluble and -insoluble fractions were immunoprecipitated with polyclonal anti-WSN antibodies and analyzed by SDS-PAGE. Numbers at the bottom indicate the chase time in hours. (C) Aliquots (50 μl [1/10]) of the samples in panel B were subjected to Western blot analysis for actin. Note that essentially the same amount of actin was present in all samples.

tance to TX-100 extraction. Accordingly, WSN-infected MDBK cells at 6.5 h p.i. were pulse-labeled and chased as described in Materials and Methods. The labeled cells were fractionated into TX-100-soluble and -insoluble fractions, immunoprecipitated with anti-WSN virus polyclonal antibodies, and subjected to SDS-PAGE analysis (Fig. 2B). The results show that immediately after synthesis, the M1 protein was present predominantly in the TX-100-soluble fraction (lanes 0.0) and that during the chase, a population of the M1 protein acquired resistance to TX-100 extraction with a $t_{1/2}$ of 20 min. The maximum amount of M1 that became resistant to TX-100 extraction was about 70 to 80% and was seen within 45 min of chase (Fig. 2B, lanes 0.75). NP, on the other hand, became resistant to TX-100 extraction faster than M1, because a significant amount of NP became TX-100 insoluble within 15 min of pulse-labeling and the level of TX-100 insolubility of NP essentially remained the same during the chase. Again, HA was essentially completely TX-100 soluble immediately after the pulse, and with the chase only the higher-molecular-weight HA became TX-100 insoluble. During the later chase period of 1.5 and 2.0 h (Fig. 2B, lanes 1.5 and 2.5), the signal for the higher-molecular-weight HA became less discernible as it was cleaved into HA1 and HA2 and/or released in virus particles. The kinetics of TX-100 insolubility for M1 and NP were essentially similar to the above when monoclonal anti-M1 and anti-NP antibodies were used for immunoprecipitation (data not shown).

We also examined the actin content of the same TX-100-soluble and -insoluble fractions used in Fig. 2B by Western blot analysis with anti-actin antibodies. The actin content was essentially the same in all samples, with an equal distribution between soluble and insoluble fractions. These internal actin controls also demonstrated the consistency of the extraction procedure (Fig. 2C). Interestingly, NS1 was detected predominantly in TX-100-insoluble fractions (Fig. 2B). However, again since no anti-NS1 antibody was present in the whole-virus antibodies, the TX-100 insolubility of NS1 protein observed here was due to its possible interaction with another TX-100-insoluble viral component. The kinetics of the TX-100 insolubility of NS1 with anti-NS1 antibodies were not determined. To investigate if viral proteins became TX-100 insoluble in another permissive cell line, we performed pulse-chase experiments with WSN-infected MDCK cells. The results show that viral proteins including HA, NP and M1 also became TX-100 insoluble after a 90-min chase (see Fig. 6C), as above in MDBK cells.

The acquired resistance of influenza virus proteins to TX-100 extraction could be due to their association with cytoskeletal components via protein-protein interaction or their association to TX-100-insoluble lipids (5, 39, 67). Therefore, to determine the cause of the TX-100 insolubility of viral proteins, WSN-infected MDBK cells were pulse-labeled at 7 h p.i. and chased for 60 min as above and extracted with a number of detergents. The results indicated that upon extraction with TX-100, Triton X-114 (TX-114), 3-[(3-cholamidopropyl)dimethylammonio]-1-propanesulfonate (CHAPS), or octylglucoside (OG), over 50% of M1, NP, and NS1 remained resistant to extraction at the end of 1 h of chase (Fig. 3). HA, on the other hand, exhibited a different profile with OG extraction (Fig. 3, lanes O.G.). The high-molecular-weight HA which exhibited TX-100 resistance after 60 min of chase remained resistant to CHAPS and TX-114 but became totally soluble to OG extraction. Again, analysis of actin in the same soluble and insoluble samples showed an equal distribution between soluble and insoluble fractions (Fig. 3, bottom panel).

These results indicate that the TX-100 insolubility of M1,

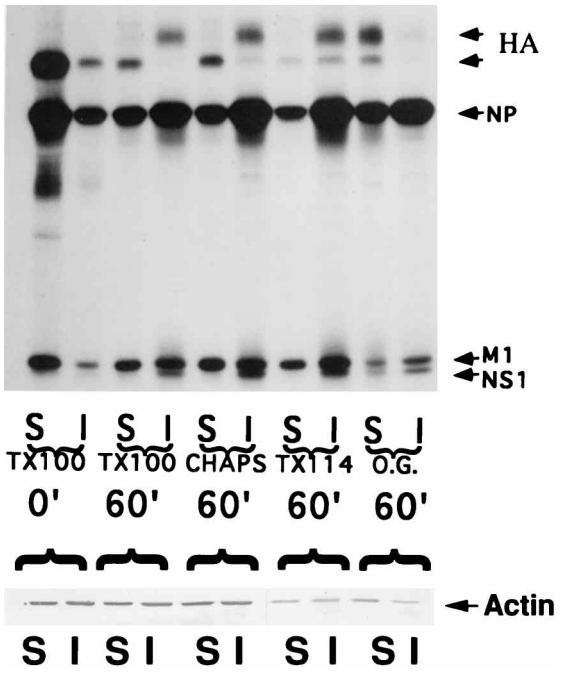

FIG. 3. Differential detergent extraction of WSN-infected MDBK cells. Infected MDBK cells at 7 h p.i. were labeled for 15 min and chased for 60 min as described in Materials and Methods. EB containing various detergents (TX-100, TX-114, CHAPS, and OG was used to extract the monolayers. Samples were immunoprecipitated with anti-WSN polyclonal sera and subjected to SDS-PAGE (10% polyacrylamide). The bottom panel shows the Western analysis of S and I fractions analyzed for actin distribution as described in the legend to Fig. 2. Chase times in min are noted at the bottom of the fluorograph.

NS1, and NP was due predominantly to protein-protein interaction with cytoskeletal components whereas the TX-100 insolubility of HA was probably due to its interaction with TX-100-insoluble lipids such as glycosphingolipids. Furthermore, we have previously shown that influenza virus NA also acquired TX-100 insolubility because of its interaction with TX-100-insoluble lipids and that this lipid-protein interaction played an important role in apical sorting of a type II transmembrane protein (28), as has been reported for glycosyl phosphatidylinositol (GPI)-anchored apical proteins (5).

The cellular distribution and localization of M1 and NP in WSN-infected MDBK cells were examined by indirect immunofluorescence. Accordingly, WSN-infected MDBK cells at 7.0 h p.i. were stained for actin filaments, intermediate filaments, and microtubules as well as for M1 and NP. The results show that late in the infectious cycle, M1 and NP exhibited distinct morphology but similar cellular distribution. At 7 h p.i., both M1 and NP were predominantly cytoplasmic (Fig. 4), as has been observed previously (55, 72). M1 exhibited diffuse and homogeneous staining, whereas NP exhibited punctuate and granular staining throughout the cytoplasm (Fig. 4, panels 1 and 7). Both M1 and NP exhibited characteristic staining at the leading edge of cells (panels 1 and 7, large arrowheads), invariably present in all WSN-infected cells, and these leading edges were also enriched in actin filaments (panels 3 and 8, large arrowheads). However, it should be noted that not all leading edges containing enriched actin filaments exhibited staining for NP (panels 7 and 8, small arrowhead) or M1 (data not shown). These results demonstrate that the observed colocalization of M1 and NP with actin filaments was not due to leaking of fluorescein and rhodamine stains through the filters. Also, some of the punctate NP staining could be seen colocalized with microfilaments (data not shown). However, except along the leading edge, the colocalization of M1 and actin filaments could not be demonstrated because of the diffuse and homogeneous staining of M1 throughout the cytoplasm. Also, since 100% of M1 (or NP) was not bound to cytoskeleton (Fig. 2), unbound soluble M1 would mask the colocalization of M1 to microfilaments when stained by immunofluorescence. Also, immunofluorescence staining following detergent extraction was very inefficient for both actin and viral proteins (data not shown). However, when the distribution of actin filaments was disrupted with cytochasin D treatment, actin showed a characteristic intracellular clumping throughout the cytoplasm, extending to the periphery of cells (Fig. 4, panel 6), as has been reported previously (7). Following cytochalasin D treatment, M1 in virus-infected cells also showed drastic morphological alteration, changing from a homogeneous (in untreated cells) to clumping (panel 5) distribution, which colocalized with the actin distribution (panel 6). NP also showed a similar distribution and colocalized with actin after cytochalasin D treatment, which was particularly discernible toward the periphery of the cells (panels 10 and 11, arrowheads). Unlike the microfilaments, neither the intermediate filaments (vimentin) nor the microtubules (tubulin) extended to the periphery of cells; therefore, they were unlikely to be involved in interacting with either M1 or NP, both of which were present, particularly at the leading edge of the cell periphery. Furthermore, viral infection at least up to 7 h p.i. did not alter the morphological distribution of microfilaments, intermediate filaments, or microtubules (data not shown). Also, under our extraction conditions at 4°C, more than 95% of the microtubules were extracted in the soluble fraction, although more than 50% of M1 remained insoluble (Fig. 5). Also, when microtubules were stabilized with Taxol or disrupted using nocodazole, there was no increase or decrease in the distribution of M1 or NP in TX-100-soluble and -insoluble fractions (data not shown). These morphological and biochemical data, taken together, support the notion that M1 and NP in WSN-infected cells interacted predominantly with microfilaments and not with microtubules or intermediate filaments, although some interactions of either of these cytoskeletal elements with viral proteins could not be ruled out.

M1 requires other viral component(s) to acquire TX-100 insolubility. To determine if WSN M1 and NP proteins alone were capable of interacting with the host cytoskeletal elements and thus becoming TX-100 resistant in the absence of other influenza virus proteins, we transiently expressed M1 and NP by using recombinant vaccinia virus in HeLa and MDCK cells or made stable MDCK cells expressing M1 under an inducible promoter (28). These experiments were done in HeLa and MDCK cells because MDBK cells are not permissive for vaccinia virus and are highly sensitive to the toxicity of $CdCl_2$ used for induction. When M1 was expressed alone by using recombinant vaccinia virus in HeLa cells, M1 remained soluble and did not become resistant to TX-100 extraction after a 90-min or longer chase (Fig. 6). Similar results were obtained using recombinant vaccinia viruses in MDCK cells (data not shown). However, the expression of proteins in MDCK cells by recombinant vaccinia viruses was lower than that in HeLa cells. On the other hand, NP, as in WSN-infected cells, acquired TX-100 resistance during the pulse and remained TX-100 resistant during the chase (Fig. 6A). It is possible that vaccinia virus proteins were interfering with the polymerization of actin filaments and interaction of M1 with cellular cytoskeletal components. However, this was unlikely, since the TX-100 insolubility of influenza virus NP remained unaffected in the

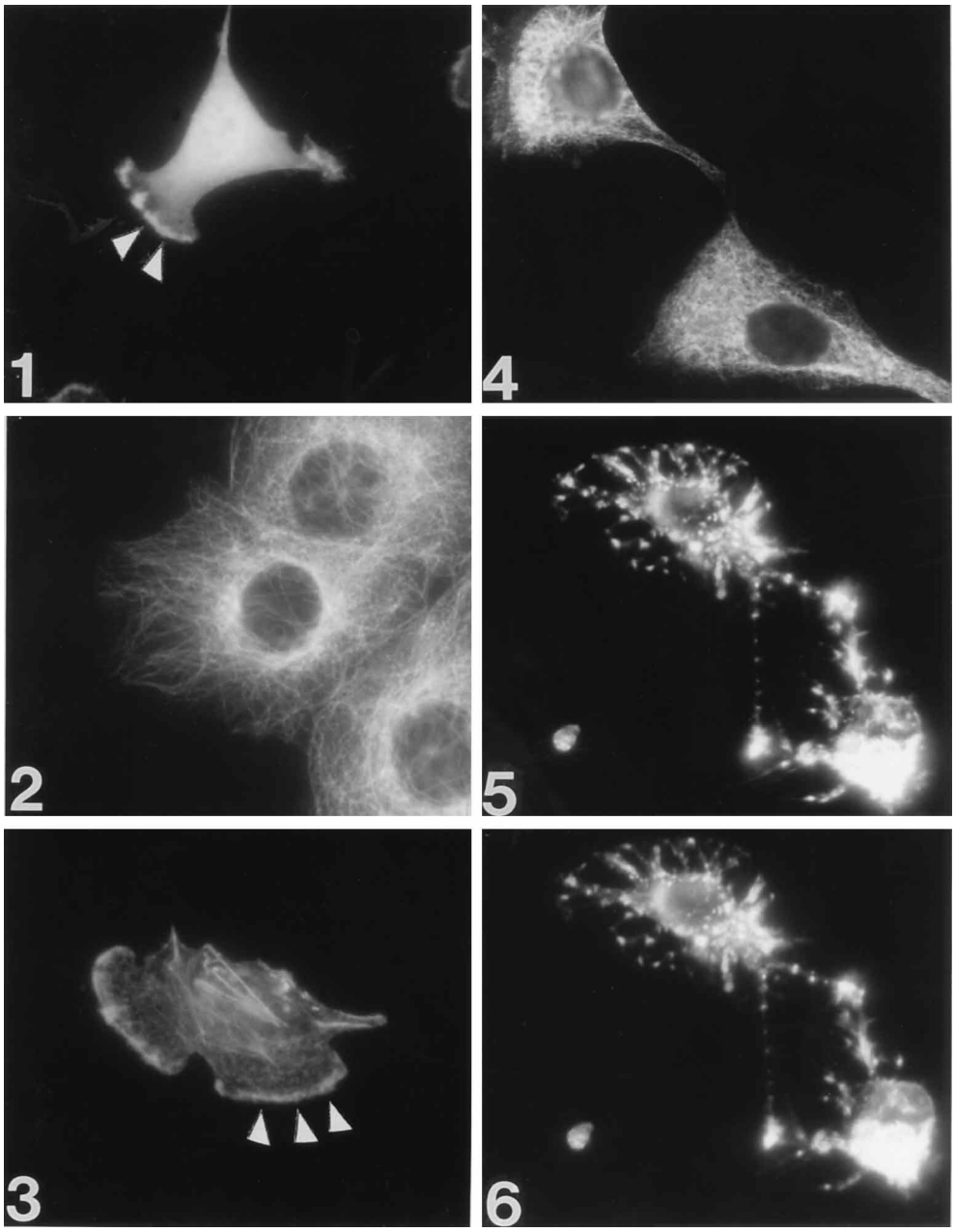

FIG. 4. Intracellular distribution of M1, NP, actin, tubulin, and vimentin in WSN-infected cells. MDBK cells were synchronously infected with of WSN virus (MOI, 10) at 4°C for 1 h. At 7 h p.i., infected cells were fixed and stained by indirect immunofluorescence. Panels: 1, anti M1; 2, anti-β-tubulin; 3, rhodamine-phalloidin; 4, anti-vimentin; 5, anti-M1; 6, rhodamine-phalloidin; 7, anti-NP; 8, rhodamine-phalloidin; 9 mock-infected, anti-M1; 10, anti-NP; 11, rhodamine-phalloidin; 12, mock-infected, anti-NP. Cells in panels 5, 6, 10, and 11 were treated with 1.0 μM of cytochalasin D for 30 min at 6.5 h p.i. before being fixed and stained. Cells in panels 5 (anti-M1) and 6 (phalloidin), panels 7 (anti-NP) and 8 (phalloidin), and panels 10 (anti-NP) and 11 (phalloidin) were costained. Note the accumulation of M1 (panel 1) and actin (panel 3) at the periphery of the cells (large arrowheads) and the codistribution of M1 (panel 5) and actin (panel 6) following cytochalsin D treatment. Also, note the colocalization (large arrowhead) of NP (panel 7) and actin filaments (panel 8) and the absence of NP (small arrowhead, panel 7) and presence of actin filaments (small arrowhead, panel 8) at the periphery of the cells. Note also the colocalization of NP (arrowheads, panel 10) and actin (arrowhead, panel 11) at the periphery of infected cells after cytochalasin D treatment.

recombinant vaccinia virus expression system (Fig. 6A), as did Sendai virus M protein expressed by recombinant vaccinia viruses (60). Finally, we examined stable cell lines of MDCK cells expressing M1 protein by using an inducible promoter for TX-100 resistance of M1. Again, the M1 expressed alone in MDCK cells did not acquire TX-100 resistance even after a total 3-h pulse-chase, whereas M1 in WSN-infected MDCK cells became TX-100 resistant only after a 90-min chase (Fig. 6C).

The above data demonstrate that M1 does not directly bind to the cytoskeleton (TX-100 insolubility) but requires interaction with other viral components to acquire TX-100 insolubility. Since M1 is likely to interact with viral RNP and since NP was observed to acquire TX-100 insolubility faster than M1 did

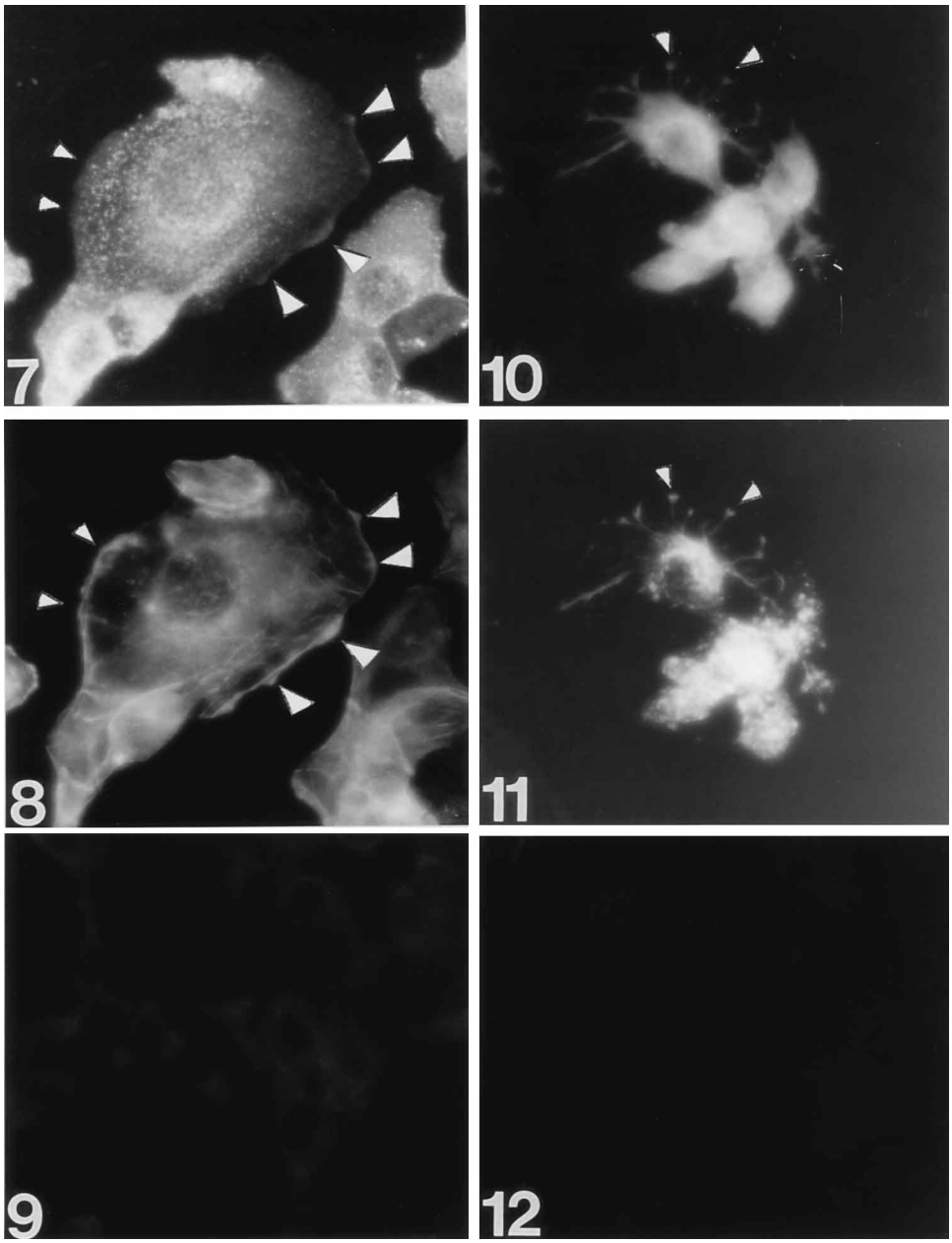

FIG. 4.—*Continued.*

in WSN-infected cells, we wanted to determine if NP was responsible for rendering M1 TX-100 insoluble. We therefore coexpressed M1 and NP by using recombinant vaccinia viruses at different MOI and determined the TX-100 insolubility after a 20-min pulse and 90-min chase. The results show that M1 did not become TX-100 insoluble when coexpressed with NP (Fig. 6B), although NP again became TX-100 resistant in coexpressing cells. The results were similar when different M1/NP ratios of recombinant vaccinia viruses were used (data not shown). Recently, Zhang and Lamb (76) reported similar results showing that influenza virus M1 acquired TX-100 insolubility in influenza virus-infected CV-1 cells but not in transfected CV-1 cells, using vaccinia virus/T7 expression for transiently expressing M1 alone or coexpressing M1 with NP or with HA, NA, and M2.

Since M1 did not acquire TX-100 insolubility when expressed alone or coexpressed with NP but both became TX-100 insoluble in influenza virus-infected cells, it is likely that M1 was acquiring TX-100 insolubility by associating with viral RNPs which in turn became bound to the cytoskeleton. Since viral RNPs are formed in the nucleus and exported in the cytoplasm at a relatively late phase of the infectious cycle, we determined the TX-100 insolubility of M1 and NP early (2 h p.i.) and late (6 h p.i.) in the infectious cycle (Fig. 7). The results show that in WSN-infected MDBK cells, M1 labeled at 2 h p.i. acquired TX-100 insolubility very inefficiently. There was no detectable TX-100 insolubility of M1 at 1 h of chase, but approximately 15% of the M1 became TX-100 insoluble after 3 h of chase (Fig. 7A) whereas at 6 h p.i. M1 acquired TX-100 insolubility with a $t_{1/2}$ of 20 min in MDBK cells (Fig.

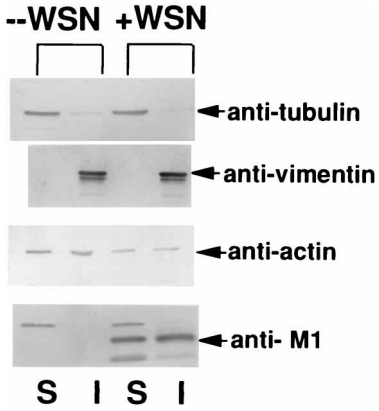

FIG. 5. Distribution of cytoskeletal proteins from TX-100-extracted mock-infected or WSN-infected MDBK cells. Mock- or WSN-infected MDBK cells at 7 h p.i. were extracted with TX-100 detergent and subjected to Western blot analysis as described previously. Soluble (S) and insoluble (I) fractions were subjected to SDS-PAGE (10% polyacrylamide) and transferred to nitrocellulose membranes. The membranes were then incubated with anti-tubulin, anti-vimentin, anti-actin, and anti-M1 monoclonal antibodies. There was no difference in the distribution of tubulin, vimentin, or actin before or after WSN-infection, and over 95% of tubulin was present in the soluble fraction.

7A). Furthermore, if the chase was continued in the presence of cycloheximide (50 μg/ml), which prevents viral protein as well as viral RNA (minus strand) and vRNP synthesis (54, 62), M1 labeled at 2 h p.i. did not become TX-100 insoluble even after 3 h of chase (Fig. 7A, lanes 180′ cx). On the other hand, at 6 h p.i., M1 became TX-100 insoluble even when incubated in the presence of cycloheximide, suggesting that M1 was interacting with preexisting vRNP in the cytoplasm. The behavior of NP essentially remained same with or without cycloheximide either early or late in the infectious cycle (data not shown). We also analyzed vRNP (minus-strand) accumulation in the cytoplasm of parallel cultures of WSN-infected MDBK cells by Northern blot analysis with plus-strand RNA as probe (Fig. 7B). At 2 h p.i. and in subsequent chase in the presence of cycloheximide, little vRNA (vRNP) was present in the cytoplasm, whereas at 6 h p.i. abundant amounts of vRNA (vRNP) were detected in the cytoplasm of WSN-infected cells. These results would support the notion that the presence of vRNA (vRNP) was a crucial factor in the M1-cytoskeleton interaction. Since NS1 is synthesized early in the infectious cycle (15, 31, 65), it is unlikely to play a major role in rendering M1 TX-100 insoluble in virus-infected cells.

M1 does not acquire TX-100 insolubility in a *ts* mutant (*ts*56) which is defective in NP at the nonpermissive temperature. *ts*56 has a defect in NP protein function at the nonpermissive temperature (39.5°C), which results in inhibiting the synthesis of cRNA and vRNA (vRNP) and secondary transcription but not primary transcription (27, 32, 63). Since NP is known to be a critical factor in switching from transcription to replication of viral RNA and vRNP synthesis, we wanted to determine if the TX-100 insolubility of M1 was affected when vRNA (vRNP) production was interfered with in *ts*56-infected cells at the nonpermissive temperature. At 5 h p.i., the TX-100 insolubility of both M1 (Fig. 8A) and NP (Fig. 8B) was similar in wild-type (WT) WSN virus-infected MDBK cells at both the permissive (33°C) and nonpermissive (39.5°C) temperatures. The rate of protein synthesis was higher at 39.5°C than at 33°C for WSN virus, as expected. At the permissive temperature, in *ts*56-infected cells, both NP and M1 exhibited a similar TX-100 resistance as in the WT WSN-infected cells (Fig. 8). At the nonpermissive temperature, both M1 and NP synthesis were reduced in *ts*56-infected cells as expected, since only primary transcription but not secondary transcription occurred in *ts*56-infected cells and the NP was localized primarily in the nucleus by immunofluorescence (data not shown). However, in *ts*56-infected cells, the NP produced at the nonpermissive temperature exhibited similar behavior to the WT NP in the WSN-

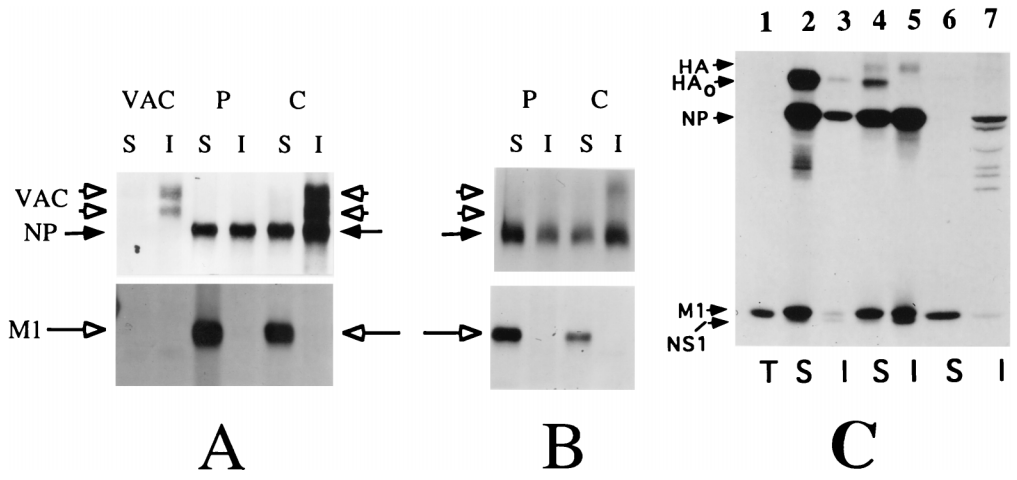

FIG. 6. TX-100 extraction of NP and M1 expressed by recombinant vaccinia virus in HeLa cells and in stable MDCK cell lines. (A) Individual expression of M1 and NP. HeLa cells were infected with recombinant vaccinia viruses (MOI, 10) expressing either M1 or NP or WT vaccinia virus. Infected cells at 5 h p.i. were pulse-labeled (lanes P) for 20 min with 200 μCi of [^{35}S]Translabel and chased (lanes C) for 3 h. Infected cells were extracted with TX-100, and soluble (S) and insoluble (I) fractions were isolated and immunoprecipitated with either anti-M1 (M1) or anti-NP (NP) monoclonal antibodies. (B) Coexpression of M1 and NP in HeLa cells. HeLa cells were coinfected with each recombinant vaccinia virus (MOI, 5) expressing M1 and NP. The cells were labeled and chased as above and extracted with TX-100 detergent. Soluble (S) and insoluble (I) samples were equally divided and immunoprecipitated with anti-M1 or anti-NP monoclonal antibodies. VAC, WT vaccinia virus. Note that some vaccinia virus proteins (VAC, open arrowheads) coprecipitated with anti-NP monoclonal antibodies and that M1 always remained TX-100 soluble, even after 3 h of chase. Similar results were obtained when cells were coinfected with M1 (MOI, 2) and of NP (MOI, 8) vaccinia viruses (data not shown). (C) M1 expression in stable MDCK cell line and WSN-infected MDCK cells. WSN-infected MDCK cells were pulse-labeled for 15 min (lanes 2 and 3) and chased for 90 min (lanes 4 and 5). MDCK stable cells lines expressing M1 (lanes 1, 6, and 7) were pulse-labeled for 90 min and chased for 90 min. Total (T, lane 1) and TX-100-soluble (S, lane 6) and -insoluble (I, lane 7) samples were immunoprecipitated with anti-WSN antibodies. M1 did not became TX-100 insoluble even after a total of pulse and chase of 3 h.

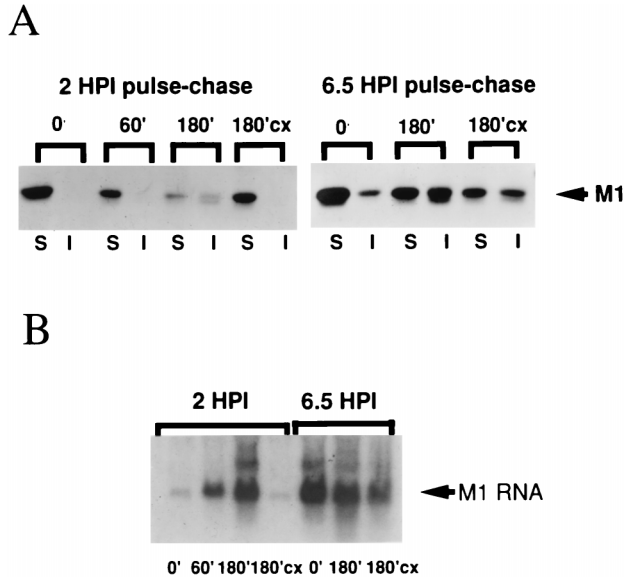

FIG. 7. TX-100 extraction of M1 protein synthesized early versus late in the virus replication cycle. (A) WSN-infected MDBK cells labeled at 2 and 6 h p.i. and chased for 3 h in the presence or absence of 1.0 mM cycloheximide. Virus-infected cells (5×10^6) were incubated at 1.5 or 6.0 h p.i. in starvation medium for 30 min. The cells were subsequently labeled with 100 μCi each of [^{35}S]Translabel and [^{35}S]cysteine for 15 min. They were then washed twice with PBS^{2+} and overlaid with prewarmed DMEM–2.5% FBS supplemented or not with 1.0 mM cycloheximide (cx) during the chase for the indicated period (in minutes). The cells were extracted with TX-100, and soluble (S) and insoluble (I) fractions were immunoprecipitated with anti-WSN polyclonal sera. (B) Total cellular RNAs from parallel WSN-infected MDBK cells in panel A were isolated and subjected to Northern blot analysis for M1 vRNA content. The blot was hybridized with a ^{32}P-labeled T7-generated riboprobe specific for M1 vRNA at 42°C overnight, in hybridization buffer containing 50% formamide. The blot was then washed under the conditions described in Materials and Methods. Note that at 2 h p.i., M1 did not became TX-100 insoluble in the presence of cycloheximide (cx) even after 3 h of chase (A) and that vRNA was not detected under these conditions (B).

infected cells and became partially TX-100 insoluble (Fig. 8B). However, M1, which was produced at the nonpermissive temperature in *ts*56-infected cells, remained predominantly TX-100 soluble (Fig. 8A, lanes 39.5°C), again supporting the idea that M1 needed vRNP in the cytoplasm to acquire TX-100 insolubility. To determine if the nonpermissive temperature rendered M1 TX-100 soluble in *ts*56-infected cells, *ts*56-infected cells were incubated and labeled at the permissive temperature (33°C) and then shifted to the nonpermissive temperature (39.5°C) during the chase. The results show that after the temperature shift, M1 acquired TX-100 insolubility (Fig. 8A, lanes 33°–39.5°C). Since earlier studies have shown that vRNA (vRNP) production is immediately stopped following the temperature shift (33), these results would suggest that M1 does not need newly synthesized vRNP to become TX-100 insoluble and can bind to preexisting vRNP in the cytoplasm. Taken together, these results would support the notion that to acquire TX-100 insolubility, M1 needs vRNP in the cytoplasm. Unlike *ts*56, a *ts* mutant of M1 (*ts*51) exhibited similar TX-100 insolubility to the wild-type M1 (data not shown), except that less M1 was present in the cytoplasm after the chase, as expected (55, 73).

DISCUSSION

Morphogenesis of influenza virus is a complex process, occurring at the plasma membrane, and involves interactions among viral structural components including the viral transmembrane proteins, matrix protein, nucleocapsid (vRNP), and host cell plasma membrane (47). How these structural viral components are brought to the site of assembly and how they interact with each other are largely unknown. The viral matrix protein (M1), presumably juxtaposed between the viral envelope and nucleocapsid, appears to play a critical role in the assembly process. A defect in M1 interferes with particle formation (74). It has been shown that late in the infectious cycle, vRNPs are exported out of the nucleus into the cytoplasm and cytoplasmic M1 prevents newly synthesized vRNPs from reentering the nucleus (72), possibly by interacting with vRNP. It was further postulated that the cytoplasmic M1-vRNP interaction facilitates the movement of vRNP to the plasma membrane, where budding takes place (72). Previous workers have shown that cytoskeletal components are involved in the transport of viral proteins and may play a role in viral morphogenesis, including the budding of enveloped viruses (4, 9, 12, 21, 24, 41, 43, 44, 71). In this study, we have examined the interaction of influenza virus proteins, particularly M1 and NP, with cytoskeletal components in infected MDBK and MDCK cell lines which are productive for WSN influenza virus infection.

Our studies, involving both morphological and biochemical analyses, show that in influenza virus-infected cells the cytoplasmic M1 and NP became associated with microfilaments whereas viral glycoproteins interacted with TX-100-insoluble lipids. In earlier studies, actin filaments were shown to interact with structural components of a number of enveloped and nonenveloped viruses. For example, M proteins of Sendai virus and Newcastle disease virus can bind actin in vitro (12). Nu-

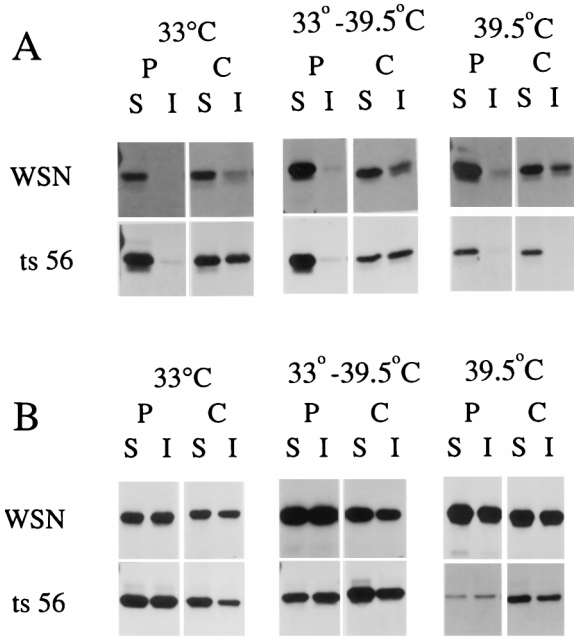

FIG. 8. TX-100 detergent extraction of *ts*56-infected MDBK cells. MDBK cells (5×10^6) were infected with *ts*56 or WT WSN virus at either 33 or 39.5°C at an MOI of 10 for 1 h and incubated for 5 h in DMEM prewarmed to 33 or 39.5°C. The cells were then starved for 30 min and pulse-labeled for 20 min with 100 μCi of [^{35}S]Translabel (P). Subsequently, they were chased in DMEM–2.5% FBS for 3 h (C). For the shift-up experiment (33 to 39.5°C), cells were pulse-labeled at 33°C and chased in DMEM prewarmed to 39.5°C. They were extracted with TX-100 as described in Materials and Methods. The samples were divided equally and immunoprecipitated with either an anti-M1 monoclonal antibody (A) or an anti-NP monoclonal antibody (B). Note that *ts*56-expressing M1 did not become TX-100 insoluble at 39.5°C even after 3 h of chase but became TX-100 insoluble at 33°C or after the shift-up to 39.5°C.

cleocapsids of murine retroviruses (44), M and NP proteins of Sendai viruses (60), and Vp1 of simian virus 40 (24) have been shown to interact with cytoskeletal elements in virus-infected cells. The present study showed that although both influenza virus M1 and NP became TX-100 resistant and appeared to associate with microfilaments in virus-infected cells, the mechanisms of their interactions appeared to be different. NP acquired TX-100 resistance during or soon after synthesis, with essentially equal efficiency in the early and late phases of the infectious cycle and when expressed alone, suggesting that NP alone can interact with cytoskeletal elements in the absence of other viral proteins. However, this is not to indicate that NP interacts directly with actin filaments, because these results cannot distinguish the NP interaction with actin from interaction with actin-associated proteins. Also, it should be noted that all cytoplasmic NP did not became TX-100 insoluble, suggesting that such interactions are dynamic and may depend on other factors and modifications (e.g., phosphorylation) affecting the state of both NP and actin. However, unlike NP, M1 behaved differently in its interaction with cytoskeletal elements. In virus-infected cells, the kinetics of M1 acquiring TX-100 resistance were slower than the kinetics of NP and varied depending on the stage of infectious cycle (i.e., slower in early stage of infectious cycle and faster in the late stage). Furthermore, M1 did not acquire TX-100 resistance when expressed alone, either using recombinant vaccinia viruses or in stable cell lines.

The above results indicate that M1 required other viral components for interacting with the host cytoskeletal elements. Among the viral components, it is unlikely that viral glycoproteins (HA and NA) are involved in mediating M1-cytoskeleton interaction, since a major fraction of M1 remained resistant to OG extraction, which rendered HA and NA completely soluble in virus-infected cells. We therefore tested NP as a possible intermediary in the M1-cytoskeleton interaction. However, upon coexpression of M1 and NP at different ratios, M1 did not acquire TX-100 resistance even after a long chase. We are therefore proposing that viral RNP rather than NP is the mediator for the M1-cytoskeleton interaction in influenza virus-infected cells. This hypothesis is also supported by the fact that M1 required a longer chase period to acquire TX-100 resistance early in the infectious cycle when the level of vRNP was low than late in the infectious cycle. Furthermore, M1 did not acquire TX-100 resistance when vRNP synthesis was suppressed early in the infectious cycle with cycloheximide (Fig. 7). Similarly, M1 did not acquire TX-100 resistance in *ts*56-infected cells at the nonpermissive temperature. *ts*56 has a defect in NP which interferes with both cRNA and vRNA (vRNP) synthesis at the nonpermissive temperature (27, 32). Again, it should be noted that the *ts* defect in NP did not interfere with its ability to interact with cytoskeletal elements (Fig. 8). Why vRNP and not NP facilitates the cytoskeletal interaction of M1 is not clear, but several possibilities exist. (i) NP in the vRNP may acquire a different conformation, which may promote M1-vRNP interaction. Although M1-vRNP complex has been observed after nonionic detergent treatment of virus particles and virus-infected cells (77), M1-NP association could not be demonstrated in coexpressing cells (data not shown). (ii) M1 may interact with vRNA of the vRNP, because it has been shown that the vRNA in the vRNP is exposed outside (2) and that M1 possesses an RNA binding site (6, 14). (iii) M1/vRNP interaction may alter the conformation of M1 so that both vRNP and M1 can interact with cytoskeletal components. It has been suggested recently that M1 may function as a bridge between vRNP and the cytoskeletal elements (72). However, our data support the reverse role of vRNP as being the mediator in the M1-vRNP-cytoskeleton interaction.

Our results that M1 alone did not stably interact with the cytoskeleton are different from an earlier observation of colocalization of M1 with actin filaments by immunofluorescence in CV-1 cells with recombinant vaccinia virus (6) but are similar to recently published data also obtained with CV-1 cells (76). Since detergent extraction was not used in earlier studies, it is possible that any M1-cytoskeleton interaction observed was sensitive to TX-100 detergent extraction and that vRNP stabilized such an interaction.

Although the mechanism of the influenza virus vRNP-cytoskeleton interaction remains unknown, an intracellular mechanism to transport specific cellular mRNA as RNP to a specific cellular compartment is well documented (20, 22, 69). These mRNAs require *cis*-acting sequences at the 3′ end to interact with the mRNA-binding proteins, forming large RNP particles which may be analogous to vRNP. These mRNA/RNP particles then interact with cytoskeleton and use either microtubule motors or actin filaments for transport to specific cellular sites for localization and translation. It will be interesting to investigate if viral RNPs use the mechanism analogous to the cellular RNP transport machinery and if some of the viral proteins provide analogous function in the transport pathway.

Although the role of cytoskeletal components in viral morphogenesis remains undetermined, a number of observations indicate that host cytoskeletal components are actively involved in different phases of the assembly and budding of enveloped viruses. Many retroviruses, including human immunodeficiency virus, bud from the leading edge of the infected cells, which are enriched in actin filaments (23, 52, 53). Similarly, other enveloped viruses, including poxviruses, measles viruses, and frog 3 viruses, also bud from actin-enriched microvilli or filopodia (4, 45). Assembly and budding of enveloped viruses require that all viral components including envelope proteins, matrix protein, and nucleocapsid must be brought to the budding site (11, 17, 47). Envelope proteins are transported to the plasma membrane via the exocytic pathway and to the apical or basolateral plasma membrane in polarized epithelial cells by using intrinsic targeting signals present in glycoproteins (37, 48, 64, 70). The role of the cytoskeleton, especially microtubules, in vesicular transport is well established (30). However, much less is known about how the viral matrix proteins and nucleocapsids are transported to the assembly site on the plasma membrane. Our studies support the notion that vRNP, as well as the M1-vRNP complex, interacts with microfilaments, which may direct these viral components to the assembly site. Furthermore, forward movement along the actin filaments may also aid in the formation of viral buds. The presence of actin in virus particles (38), protrusion of actin filaments in the measles virus buds (4), and budding of human immunodeficiency virus from one end of the cell containing concentrated actin filaments (52, 53) would support the active role of host microfilaments in viral morphogenesis. Clearly, much work is needed to elucidate the steps in viral assembly and bud formation and the role of host cytoskeletal components in this process.

ACKNOWLEDGMENTS

Work reported here was partially supported by NIAID/NIH grants AI 12729 and AI 16348.

We thank Eleanor Berlin for typing the manuscript.

REFERENCES

1. **Barak, L. S., R. R. Yocum, E. A. Nothnagel, and W. W. Webb.** 1980. Fluorescence staining of the actin cytoskeleton in living cells with 7-nitrobenz-2-

Oxa-1,3-diazole-phallacidin. Proc. Natl. Acad. Sci. U.S.A. **77:**980–984.
2. **Baudin, F., C. Bach, S. Cusack, and R. W. H. Ruigrok.** 1994. Structure of influenza virus RNP. I. Influenza virus nucleoprotein melts secondary structure in panhandle RNA and exposes the bases to the solvent. EMBO J. **13:**3158–3165.
3. **Ben-Ze'ev, A., A. Duerr, F. Solomon, and S. Penman.** 1979. The outer boundary of the cytoskeleton: a lamina derived from plasma membrane proteins. Cell **17:**859–865.
4. **Bohn, W., G. Rutter, H. Hohenberg, K. Mannweiler, and P. Nobis.** 1986. Involvement of actin filaments in budding of measles virus: studies on cytoskeletons of infected cells. Virology **149:**91–106.
5. **Brown, D. A., and J. K. Rose.** 1992. Sorting of GPI-anchored proteins to glycolipid-enriched membrane subdomains during transport to the apical cell surface. Cell **68:**533–544.
6. **Bucher, D., S. Popple, M. Baer, A. Mikhail, Y.-F. Gong, C. Whitaker, E. Paoletti, and A. Judd.** 1989. M protein (M1) of influenza virus: antigenic analysis and intracellular localization with monoclonal antibodies. J. Virol. **63:**3622–3633.
7. **Cooper, J. A.** 1987. Effects of cytochalasin and phalloidin on actin. J. Cell Biol. **105:**1473–1478.
8. **Cudmore, S., P. Cossart, G. Griffith, and M. Way.** 1995. Actin-based motility of vaccinia virus. Nature **378:**636–638.
9. **Damsky, C. H., J. P. Sheffield, G. P. Tuszynski, and L. Warren.** 1977. Is there a role for actin in virus budding? J. Cell Biol. **75:**593–605.
10. **Enami, M., and K. Enami.** 1996. Influenza virus hemagglutinin and neuraminidase glycoproteins stimulate the membrane association of the matrix protein. J. Virol. **70:**6653–6657.
11. **Gaedigk-Nitschko, K., and M. J. Schlesinger.** 1991. Site-directed mutations in Sindbis virus E2 glycoprotein's cytoplasmic domain and the 6K protein lead to similar defects in virus assembly and budding. Virology **183:**206–214.
12. **Giuffre, R. M., D. R. Tovell, C. M. Kay, and D. L. J. Tyrell.** 1982. Evidence for an interaction between the membrane protein of a paramyxovirus and actin. J. Virol. **42:**963–968.
13. **Granoff, A., and D. W. Kingsbury.** 1964. Effect of actinomycin D on the replication of Newcastle disease and influenza virus. Ciba Found. Symp. Cell. Biol. **1964:**96–115.
14. **Gregoriades, A., and B. Frangoine.** 1981. Insertion of influenza virus M1 protein into the viral lipid bilayer and localization of site of insertion. J. Virol. **40:**323–328.
15. **Greenspan, D., P. Palese, and M. Krystal.** 1988. Two nuclear localization signals in the influenza virus NS1 nonstructural protein. J. Virol. **62:**3020–3026.
16. **Griffin, J. A., and R. W. Compans.** 1979. Effect of cytochalasin B on the maturation of enveloped viruses. J. Exp. Med. **150:**379–391.
17. **Griffiths, G., and P. Rottier.** 1992. Cell biology of viruses that assemble along the biosynthetic pathway. Semin. Cell Biol. **3:**367–381.
18. **Gujuluva, C. N., A. Kundu, K. G. Murti, and D. P. Nayak.** 1994. Abortive replication of influenza virus A/WSN/33 in HeLa 229 cells: defective membrane function during entry and budding processes. Virology **204:**491–505.
19. **Hay, A. J.** 1974. Studies on the formation of the influenza virus envelope. Virology **60:**398–418.
20. **Heskett, J. E., and I. F. Pryme.** 1991. Interaction between mRNA, ribosomes and the cytoskeleton. J. Biochem. **277:**1–10.
21. **Hiller, G., K. Weber, L. Schnieder, C. Parajsz, and C. Junwirth.** 1979. Interaction of assembled progeny pox viruses with the cellular cytoskeleton. Virology **98:**142–153.
22. **Hovland, R., G. Campbell, I. Pryme, and J. Hesketh.** 1995. The mRNA for cyclin A, c-myc and ribosomal protein L4 and S6 are associated with cytoskeletal-bound polysomes in HepG2 cells. J. Biochem. **310:**193–196.
23. **Hunter, E.** 1994. Macromolecular interactions in the assembly of HIV and other retroviruses. Virology **5:**71–83.
24. **Kasamatsu, H., W. Lin, J. Eden, and J. P. Revel.** 1983. Visualization of antigens attached to cytoskeletal framework in animal cells: colocalization of simian virus 40 vp1 polypeptide and actin in TC7 cells. Proc. Natl. Acad. Sci. USA **80:**4339–4343.
25. **Klenk, H.-D., W. Wollert, R. Rott, and C. Scholtissek.** 1974. Association of influenza virus proteins with cytoplasmic fractions. Virology **57:**28–41.
26. **Klymkowsky, M. W.** 1995. Intermediate filaments: new proteins, some answers, more questions. Curr. Biol. **7:**46–54.
27. **Krug, R. M., M. Ueda, and P. Palese.** 1975. Temperature-sensitive mutants of influenza WSN virus defective in virus-specific RNA synthesis. J. Virol. **16:**790–796.
28. **Kundu, A. K., R. T. Avalos, C. N. Sanderson, and D. P. Nayak.** 1995. Transmembrane domain of influenza virus neuraminidase, a type II protein, possesses an apical sorting signal in polarized MDCK cells. J. Virol. **70:**6508–6515.
29. **Laemmli, U. K.** 1970. Cleavage of structural proteins during the assembly of the head of bacteriophage T4. Nature **227:**680–685.
30. **Lafont, F., J. K. Burkhard, and K. Simons.** 1995. Involvement of microtubule motors in basolateral and apical transport in kidney cells. Nature **372:**801–803.
31. **Lazarowitz, S. G., R. W. Compans, and P. W. Choppin.** 1971. Influenza virus structural and nonstructural proteins in infected cells and their plasma membranes. Virology **46:**830–843.
32. **Li, R., P. Palese, and M. Krystal.** 1989. Complementation and analysis of an NP mutant of influenza virus. Virus Res. **12:**97–112.
33. **Li, S., M. Xu, and K. Coelingh.** 1995. Electroporation of influenza virus ribonucleoprotein complexes for rescue of the nucleoprotein and matrix genes. Virus Res. **37:**153–161.
34. **Liu, C., and G. M. Air.** 1993. Selection and characterization of neuraminidase-minus mutant of influenza virus and its rescue by cloned neuraminidase genes. Virology **194:**403–407.
35. **Liu, C., M. C. Eichelberger, R. W. Compans, and G. M. Air.** 1995. Influenza type A virus neuraminidase does not play a role in viral entry, replication, assembly, or budding. J. Virol. **69:**1099–1106.
36. **Lohmeyer, J., L. T. Talens, and H.-D. Klenk.** 1979. Biosynthesis of the influenza virus envelope in abortive infection. J. Gen. Virol. **42:**73–88.
37. **Low, S. H., B. L. Tang, S. H. Wong, and W. Hong.** 1992. Selective inhibition of protein targeting to the apical domain of MDCK cells by brefeldin A. J. Cell Biol. **118:**51–62.
38. **Loza-Tulimowska, M., T. Michalak, and R. Semkow.** 1981. Attempts at detection of actomyosin associated with influenza virus. Acta Virol. **25:**251–253.
39. **Luna, E. J., and A. L. Hitt.** 1992. Cytoskeleton-plasma membrane interactions. Science **258:**955–964.
40. **Lydy, S. L., S. Basak, and R. W. Compans.** 1990. Host cell-dependent lateral mobility of viral glycoproteins. Microb. Pathog. **9:**375–386.
41. **Melki, R., Y. Gaudin, and D. Blondel.** 1994. Interaction between tubulin and the viral matrix protein of vesicular stomatitis virus: possible implications in the viral cytopathic effect. J. Virol. **202:**339–347.
42. **Mitnaul, L. J., M. R. Castrucci, K. G. Murti, and Y. Kowaoka.** 1996. The cytoplasmic tail of influenza a virus neuraminidase (NA) affects NA incorporation into virions, virion morphology, and virulence in mice but is not essential for virus replication. J. Virol. **70:**873–879.
43. **Morrison, T. G., and L. J. McGinnes.** 1985. Cytochalasin D accelerates the release of Newcastle disease virus from infected cells. Virus Res. **4:**93–106.
44. **Mortara, R. A., and G. I. E. Koch.** 1989. An association between actin and nucleocapsid polypeptides in isolated murine retroviral particles. J. Submicrosc. Cytol. Patho. **21:**295–306.
45. **Murti, K. G., M. Chen, and R. Goorha.** 1985. Interaction of frog virus 3 with the cytomatrix III. Role of microfilaments in virus release. Virology **142:**317–325.
46. **Naim, H. Y., and M. G. Roth.** 1993. Basis of selective incorporation of glycoproteins into the influenza virus envelope. J. Virol. **67:**4831–4841.
47. **Nayak, D. P.** 1996. A look at assembly and morphogenesis of orthomyxo-and paramyxoviruses. ASM News **62:**411–414.
48. **Nayak, D. P., and M. A. Jabbar.** 1989. Structural domains and organizational conformation involved in sorting and transport of the influenza virus transmembrane proteins. Annu. Rev. Microbiol. **43:**465–501.
49. **Ojakian, G. K., and R. Schwimmor.** 1988. The polarized distribution of an apical cell surface glycoprotein is maintained by interactions with the cytoskeleton of Madin-Darby canine kidney cells. J. Cell Biol. **107:**2377–2387.
50. **Patterson, S., J. Gross, and J. S. Oxford.** 1988. The intracellular distribution of influenza virus matrix protein and nucleoprotein in infected cells and their relationship to hemagglutinin in the plasma membrane. J. Gen. Virol. **69:**1859–1872.
51. **Pattnaik, A. K., D. J. Brown, and D. P. Nayak.** 1986. Formation of influenza virus particles lacking hemagglutinin on the viral envelope. J. Virol. **60:**994–1001.
52. **Pearce-Pratt, R., D. Malamud, and D. M. Phillips.** 1994. Role of the cytoskeleton in cell-to-cell transmission of human immunodeficiency virus. J. Virol. **68:**2898–2905.
53. **Perotti, M.-E., X. Tan, and D. M. Phillips.** 1996. Directional budding of human immunodeficiency virus from monocytes. J. Virol. **70:**5916–5921.
54. **Pons, M. W.** 1973. The inhibition of influenza virus RNA synthesis by actinomycin D and cycloheximide. Virology **51:**120–128.
55. **Rey, O., and D. P. Nayak.** 1992. Nuclear retention of M1 protein via temperature-sensitive mutant of influenza virus (A/WSN/33) does not affect nuclear export of viral ribonucleoproteins. J. Virol. **66:**5815–5824.
56. **Rindler, M. J., I. E. Ivanov, and D. D. Sabatini.** 1987. Microtubule-acting drugs lead to the nonpolarized delivery of the influenza hemagglutinin to the cell surface of polarized Madin-Darby canine kidney cells. J. Cell Biol. **104:**231–241.
57. **Rutter, G., and K. Mannweiler.** 1977. Alterations of actin-containing structures in BHK21 cells infected with Newcastle disease virus and vesicular stomatitis virus. J. Gen. Virol. **37:**233–242.
58. **Sambrook, J., E. F. Fritsch, and T. Maniatis.** 1989. Molecular cloning: a laboratory manual, 2nd ed. Cold Spring Harbor Laboratory Press, Cold Spring Harbor, N.Y.
59. **Sanders, M. C., and Y.-I. Wang.** 1990. Exogenous nucleation sites fail to induce detectable polymerization of actin in living cells. J. Cell Biol. **110:**359–365.
60. **Sanderson, C. M., R. Avalos, A. Kundu, and D. P. Nayak.** 1995. Interaction of Sendai viral F, HN, and M protein cytoskeletal and lipid components in

Sendai virus-infected BHK cells. Virology **209:**701–707.
61. **Sanderson, C. M., H.-H. Wu, and D. P. Nayak.** 1994. Sendai virus M protein binds independently to either the F or the HN glycoprotein in vivo. J. Virol. **68:**69–76.
62. **Scholtissek, C., and R. Rott.** 1970. Synthesis in vivo of influenza virus plus and minus strand RNA and its preferential inhibition by antibiotics. Virology **40:**989–996.
63. **Scholtissek, C., R. Kruczina, R. Rott, and H.-D. Klenk.** 1974. Characteristics of an influenza mutant temperature-sensitive for viral RNA synthesis. Virology **58:**317–322.
64. **Sheshberadaran, H., and R. A. Lamb.** 1991. Simian virus 5 membrane protein maturation: expression in virus-infected cells and from an eukaryotic vector. Virology **183:**803–809.
65. **Skehel, J. J.** 1973. Early polypeptide synthesis in influenza virus-infected cells. Virology **56:**394–399.
66. **Skibbens, J. E., M. G. Roth, and K. S. Matlin.** 1989. Differential extractability of influenza virus hemagglutinin during intracellular transport in polarized epithelial cells and nonpolar fibroblasts. J. Cell Biol. **108:**821–832.
67. **Stephen, J. N., and C. M. Isacke.** 1993. The cytoplasmic tail of CD44 is required for basolateral localization in epithelial MDCK cells but does not mediate association with the detergent-insoluble cytoskeleton of fibroblasts. J. Cell Biol. **121:**1299–1310.
68. **Sun, H-Q., K. Kwiatkowska, and H. L. Yin.** 1995. Actin monomer binding proteins. Curr. Biol. **7:**102–110.
69. **Sundell, C. L., and R. H. Singer.** 1991. Requirement of microfilaments in sorting of actin messenger RNA. **253:**1275–1277.
70. **Sveda, M. M., L. J. Markoff, and C.-J. Lai.** 1984. Influenza virus hemagglutinin containing an altered hydrophobic carboxy terminus accumulates intracellularly. J. Virol. **49:**223–228.
71. **Tashiro, M., J. T. Seto, H.-D. Klenk, and R. Rott.** 1993. Possible involvement of microtubule disruption in bipolar budding of a Sendai virus mutant, F1-R, in epithelial MDCK cells. J. Virol. **67:**5902–5910.
72. **Whittaker, G., M. Bui, and A. Helenius.** 1996. Nuclear trafficking of influenza virus ribonucleoprotein in heterokaryons. J. Virol. **70:**2743–2756.
73. **Whittaker, G., I. Kemler, and A. Helenius.** 1995. Hyperphosphorylation of mutant influenza virus matrix protein, M1, causes its retention in the nucleus. J. Virol. **69:**439–445.
74. **Yasuda, J., D. J. Bucher, and A. Ishihama.** 1994. Growth control of influenza A virus by M1 protein: analysis of transfectant viruses carrying the chimeric M gene. J. Virol. **68:**8141–8146.
75. **Ye, Z., D. Robinson, and R. R. Wagner.** 1995. Nucleus-targeting domain of the matrix protein (M_1) of influenza virus. J. Virol. **69:**1964–1970.
76. **Zhang, J., and R. A. Lamb.** 1996. Characterization of membrane association of the influenza virus matrix protein in living cell. Virology **225:**255–266.
77. **Zhirnov, O. P.** 1992. Isolation of matrix protein M1 from influenza viruses by acid-dependent extraction with nonionic detergent. Virology **186:**324–330.